J Mater Sci (2007) 42:3783–3788
DOI 10.1007/s10853-006-0414-z

Radar wave absorbing characterization of bicomponent fibers

Bin Yu · Lu Qi · Hui Sun · Jian-zhong Ye

Received: 1 March 2006 / Accepted: 5 May 2006 / Published online: 11 February 2007

Abstract The sheath–core bicomponent fibers were melt-spun by co-extrusion of polypropylene and polypropylene/fillers master-batches. The melt-spun fibers were characterized by DSC, SEM and MSERA. Crystallinity of bicomponent fibers with wave absorption agent was more than that of PP alone. SEM results showed that inorganic particles in fibers had relatively good dispersibility. The electrical resistance of fibers containing bronze particles in the core part reached minimum at the 20 Wt% bronze content. Fibers with ferrite/bronze showed the good radar absorption effects and the absorption property was improved with the increase in bronze content. The fiber having the ferrite or ferrite/bronze in the core-part exhibited the lower reflectivity compared the fiber with ferrite or ferrite/bronze in the sheath-part.

Introduction

The radar signal strength, scattered from a target, determines its detectability. This pertains to the radar cross section (RCS), which frequently should be reduced. Radar-absorbing material (RAM) is a very effective means of RCS reduction in the context of camouflage technology. The basic design theories of RAM, such as Salisbury screen theory, Jaumann absorber theory, etc. were published from early 1950s onwards. But these theoretical studies abated, recently, the main research topic being transferring toward the development of loss material [1, 2]. There are electro loss and magnetic loss materials having different advantages and disadvantages of each which can be used as a mixture [3]; however, the magnetic loss material and coating materials [4] are usually base one, heavy weight of the material is still a concerning problem. To remedy this problem, the more and more researches about RAM have been concentrated on fibers materials [5, 6]. A number of researches have been carried out, which include spinning of electrically conducting fibers [7], coating fibers with electrically conducting materials such as metals [8] or conducting polymers and textiles coated with conducting polymers [9, 10].

However, to the best of our knowledge, there are no reported experimental results on the design of bicomponent fibers RAM by compound spinning. In this paper, we studied how to design a inorganic–organic radar absorbing fibers. For the purpose, we have prepared a bicomponent fiber with sheath–core structure using PP chips and various fillers.

B. Yu · L. Qi (✉) · J.-z. Ye
Research Institute of Biological and Spinning Materials, Tianjin Polytechnic University, Tianjin 300160, China
e-mail: suhui7712@163.com

H. Sun
School of Materials Science and Engineering, Tianjin University, Tianjin 300072, China

Experimental

Materials

Ferrite provided from Beijing Central Iron & Steel Research Institute and rich bronze powder supplied by Wuxi Gold Powder Factory were used as radar

absorbing agents. The mean diameter of all the radar absorbing agents was approximately 3 micrometer. Each type of specimen is denoted by the particles contents by weight and volume percentage in core-part and sheath-part of the fibers as shown in Table 1. Polypropylene chips (isotactic PP) was provided from Shanghai PetroChemical Co. Ltd, China. Its characteristics commonly used for fibers spinning are as follows; Mn: 1.7×10^5, MI: 39.0 g/10 min, Density: 0.92 g/cm^3, and Poly-dispersity: 3.8. For easier spinning process, PP/fillers master-batches were prepared by a conventional twin-screw extruder.

Spinning process and machine

The spinning machine was a general conjugate spinning machine, which was composed of two extruders (L/D = 25, D = 20 mm) and gear pumps. The spinning processes were performed by two different methods. In the first process, the PP/ radar absorbing agents master-batches were added into the core-part and PP chips were added into the sheath-part. For the second process, the PP/ radar absorbing agents master-batches were put into the sheath-part and the PP chips were put into core-part. Both core-part master-batches and sheath-part master-batches were dried for at least 2 h at 100 °C in vacuum drier to secure complete moisture-free state. The fibers sheath–core ratio was 40/60(W/W) controlled through adjustment of the speed of gear pumps. Two kinds of master-batches were melted in both cylinders, combined in the spinneret. They were extruded through the mono-nozzles, which have diameter of 0.4 mm at the first spinning process and 0.8 Φ mm at second.

The Fig. 1 illustrates the spinning system used for generating sheath–core bicomponent fibers. The processing temperatures are listed in Table 2.

Thermal analysis

For thermodynamic experiment, dynamic scanning calorimerer (DSC, Perkin–Elmer DSC-7) equipped with a cooler was used under the nitrogen atmosphere. All the samples were heated from 0 to 250 °C at 10 °C/min. From this procedure, the melting temperature

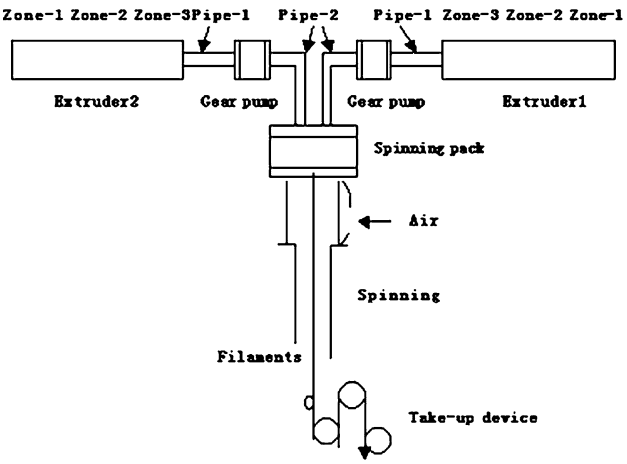

Fig. 1 Schematic diagram for the bicomponent fibers spinning system

(T_m) of the fibers was obtained and apparent enthalpies of fusion were calculated from the area of the endothermic peak. The percent crystallinity of polypropylene was evaluated using the following equation:

$$\text{crystallinity}\,(\%) = \frac{\Delta H_f}{\Delta H_f^0 \cdot \omega_f} \quad (1)$$

where ΔH_f is the heat of fusion of PP fibers, ω_f is the weight fraction of PP in the blends, and ΔH_f^0 is the extrapolated value of the enthalpy corresponding to the heat of fusion of 100% crystalline PP taken as 209 kJ/kg from the literature [11].

Morphology observation

The cross-section structure of the sheath–core bicomponent fibers was observed using Scanning Electron Microscope (SEM, Hitachi 450). The SEM samples were goldsputtered before observation.

Electro characterization permittivity and permeability of the fiber

The electrical resistance of the bicomponent fibers test were performed using fiber mass specific electrical resistance apparatus (MSERA, YG321) at 25 °C, 65HR%.

Table 1 Specimen denotations of bicomponent fibers

	PS0	PC0	C20S0	C40S0	C0S20	C0S40
Contents of particle in the core-part of the fibers (Wt%/Vol%)	0		20/5.01	40/12.38	0	0
Contents of particle in the sheath-part of the fibers (Wt%/Vol%)	0		0	0	20/5.01	40/12.38

Note: C means the core-part, S means the sheath-part

Table 2 Processing temperature (°C) for generating sheath–core bicomponent fibers (refer to Fig. 1 for illustration)

	Pack	Pipe-2	Gear pump	Pipe-1	Clamp	Zone-3	Zone-2	Zone-1
Temperature (°C)	255	250	240	240	240	240	240	150

Performance test of radar absorbing

The performance test of radar absorbing was evaluated by reflectivity using Arch method. Reflectivity R is ratio of RAM reflective power to metallic plate reflective power, which can be expressed as:

$$R = \frac{P_a}{P_m} \tag{2}$$

where P_a is the reflective power of the sample and P_m is the reflective power of metallic plate.

In practice, we surveyed the ratio of the reflective power of the sample and the reflective power of metallic plate to the same reference signal that was in direct proportion to the transmit respectively.

$$R_m = \frac{P_m}{P_i}, R_a = \frac{P_a}{P_i} \tag{3}$$

where P_i is reference signal. So

$$R = \frac{P_a}{P_m} = \frac{P_a/P_i}{P_m/P_i} = \frac{R_a}{R_m} \tag{4}$$

the reflectivity was finally expressed with db as:

$$R_{db} = 10 \lg R_a - 10 \lg R_m. \tag{5}$$

The schematic diagram of the experimental setup was shown in Fig. 2. The reflectivity of the samples were measured and compared with that from a plane metallic plate. Measurement was carried out using an HP 8757E network analyzer in the swept frequency range from 2 to 18 GHz. All fiber samples were made 180 mm × 180 mm needle-punched nonwoven with 2.5 mm thickness and 380 g/m^2 surface density by DILO needle-punched machine in order to cover the metallic plate.

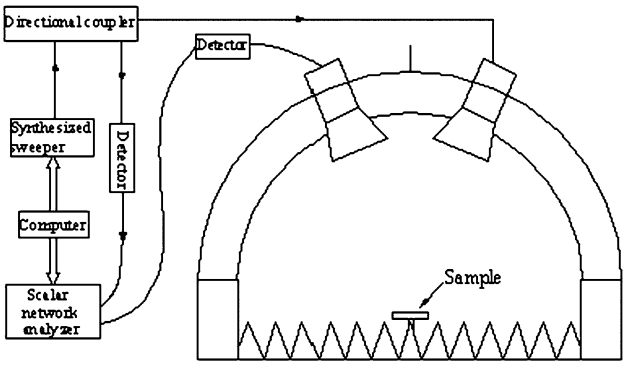

Fig. 2 Reflectivity measurement setup of arch method

The test of the mechanical properties of the fibers

The breaking stress was tested by fiber electron mechanical instrument (YG003A) with the descendent velocity of 5 mm/min, and pre-strain was 200 g.

Result and discussion

Thermal property

Differential scanning calorimetry thermograms of all the fibers are depicted in Fig. 3. Figure 3(a) shows three curves of the DSC thermogram profile of fibers containing various content ferrite and bronze in the core-part. Figure 3(b) shows three curves of fibers containing various content ferrite and bronze in the sheath-part. Table 3 summarizes the data from DSC. There was a negligible relationship between the melting point of fibers and the variation of fillers content in the case of the fibers with added fillers in the core-part and in the sheath-part. In DSC graphs, the peak area of melting point (T_m) of fibers including ferrite and bronze was slightly higher than that of the pure PP fibers (samples PS0 and PC0) and the crystallinity of PP fiber including ferrite and bronze particles increased slightly (Table 3). The wt% crystallinity of PP was calculated via the standard heat of crystallization which was taken to be 209 J g^{-1}. Recently, Sang and Sung [12] reported that the addition of the silver made the crystallinity of fibers reduce. However, in case of our results, the behavior of PP crystallization in the matrix led to a different result. The increase in crystallinity of PP revealed that the ferrite and bronze particles made for the crystallization of PP. Thus we supposed that ferrite and bronze particles in the PP matrix acted not as impurities but as nucleating agents.

Cross sections of fibers observation

SEM is a good way to present a real-space image of the particles filled in the polymer materials. Hence, the

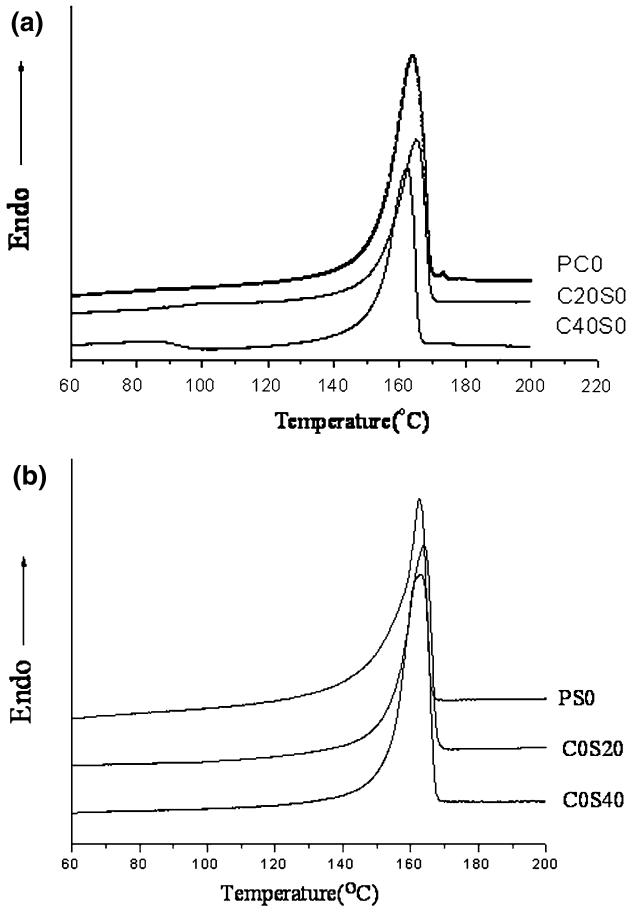

Fig. 3 DSC of spun fibers containing ferrite and bronze in core-part (**a**) and in the sheath-part (**b**)

cross-section of bicomponent fibers was observed on SEM. In Fig. 4, SEM micrograph shows the cross-sections of core-part filled with (a) the 20% bronze/ferrite and (b) the 40% bronze/ferrite particles. In Fig. 4(b), many conglomerations of the particles and holes were observed. The SEM photograph of core-part filled with 20% bronze/ferrite has seldom conglomeration and hole in Fig. 4(a). It was demonstrated that the compatibility of the PP with the particles become bad with the content of particles increase which will affect the mechanical and electro properties of the fibers.

Table 3 The results of DSC

Sample	Melting point T_m (°C)	Heat of fusion (J g^{-1})	Crystallinity of PP (%)
PC0	164.02	109.40	52.15
C20S0	164.95	117.46	56.20
C40S0	162.05	115.23	55.13
PS0	164.12	108.89	52.10
C0S20	164.72	117.82	56.37
C0S40	162.79	119.85	57.34

The electrical resistivity of the fibers

The mass specific electrical resistivity (MSER) of fibers filled with bronze particles is shown in Fig. 5. It was obvious that the MSER of fibers reduced at the low bronze content, but it began to increase after the metal content reached 20%. This can be explained by the non-homogeneous morphological structure of the fibers with various content fillers. Two phases exist: bronze particles and PP regions. As Faez et al. [13] previously reported, a degree of connectivity between the conductive additives must exist in order to facilitate the electro conduction. The connectivity between the bronze particles began to form among the PP with the addition of bronze particles. So the MSER reduced rapidly. But too many bronze particles will make the compatibility of bonze with PP become bad (as shown in Fig. 4) and some bronze particles may conglomerations resulting to the connection between bronze particles breaking and MSER increase.

The radar wave absorption properties of the fibers

The Fig. 6 shows the wave absorption properties of fibers, which were filled ferrite, ferrite/15Wt% bronze and ferrite/20Wt% bronze respectively in the core-part. The result showed that the fibers with ferrite/bronze had low reflectivity and wide absorption bandwidth compared with fibers with single ferrite. The reflectivity of the fiber decreased with the bronze content increasing. This can be explained by the following two reasons. On one hand, the conductance was increased that resulting to the electric loss increasing with the addition of bronze particles, as shown in Fig. 5. On the other hand, the bronze particles cooperate with the ferrite should also explain the reasonable absorption. As we all known, the Raleigh scattering will happen when the incident electromagnetic wave with the wavelength far bigger than the particles size impinged on the smaller particles. The bronze particles size was about 10^{-6} m, while the radar wavelength from 3.75×10^{-2} m to 1.67×10^{-2} m (8–18 GHz). So the rayleigh scattering was going to happen when the radar impinged on the metal particles. The widespread and almost isotropy rayleigh scattering waves were absorbed uniformly by the ferrite in all directions. So the input bronze particles in the fibers made the absorption wave performance improved. But too many bronze did not necessary. It was because that the mechanical properties of the fibers decreased rapidly and the fibers cannot be spun even when the content of fillers reached the certain value, as we can see from the Fig. 7. Besides, the MSER of fibers with very higher bronze content increased rapidly.

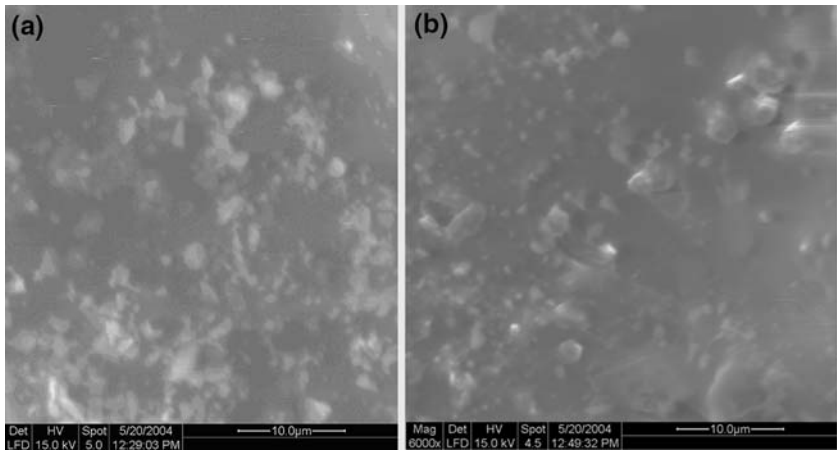

Fig. 4 SEM photographs (×6.00 k) of the core-part of (**a**) C20S0 and (**b**) C40S0

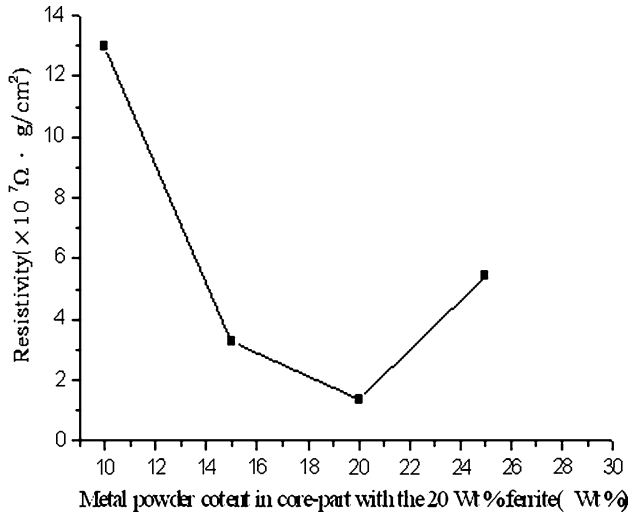

Fig. 5 The relation of MSER of fibers and the bronze metal particles content

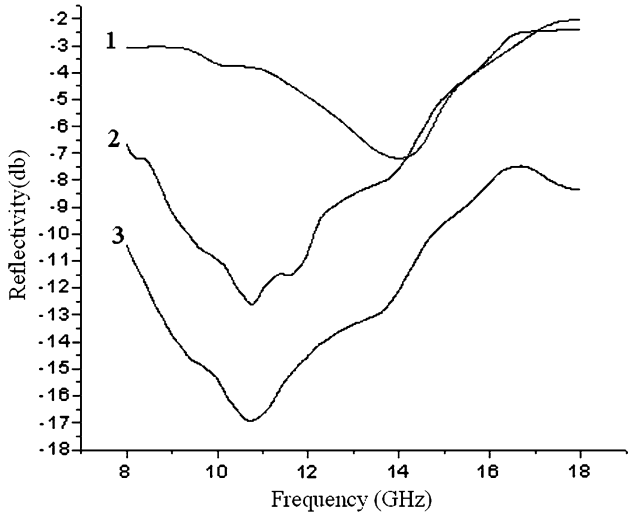

Fig. 6 The effect of fillers on the reflectivity of fiber 1: fiber with ferrite; 2: fiber with ferrite/15Wt% bronze; 3: fiber with ferrite/20Wt% bronze

The Figs. 8 and 9 indicate the effect of spinning processes on the wave absorbing property of the fibers. The result shows that the fiber with the ferrite or ferrite/bronze in the core-part exhibited the lower reflectivity than the fiber with the ferrite or ferrite/bronze in the sheath-part. The reason can be closely explained as following. When the fillers were filled into the sheath-part, the permittivity and permeability of sheath-part increased rapidly that was bad for the entry of the radar wave and the sheath-part of the fiber generated much reflective wave which resulted the reduce of the absorbing property. At the other spinning process, it was easy for the radar wave to go into the inner of the fiber and attenuation because the sheath-part of the fiber was with lower the permittivity and permeability. So the fiber with the fillers in the core-part have good absorbing property compared with the fiber with the fillers in the sheath-part.

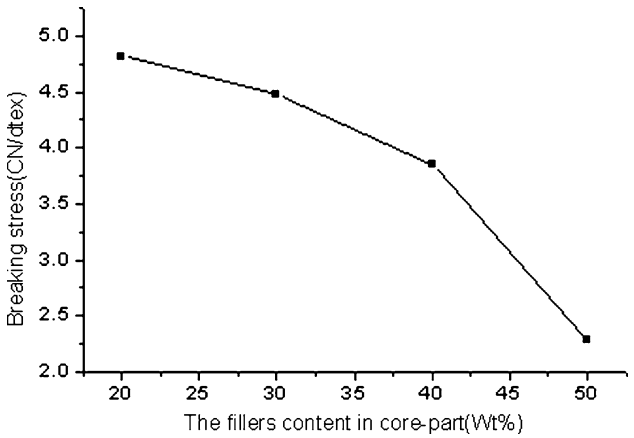

Fig. 7 The change of breaking stress with the fillers content increase

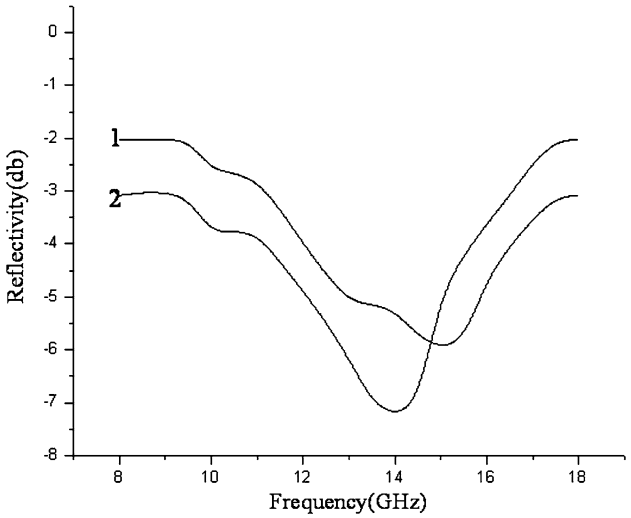

Fig. 8 The effect of spinning processes on the reflectivity of fiber 1: with ferrite in the sheath-part; 2: with ferrite in the core-part

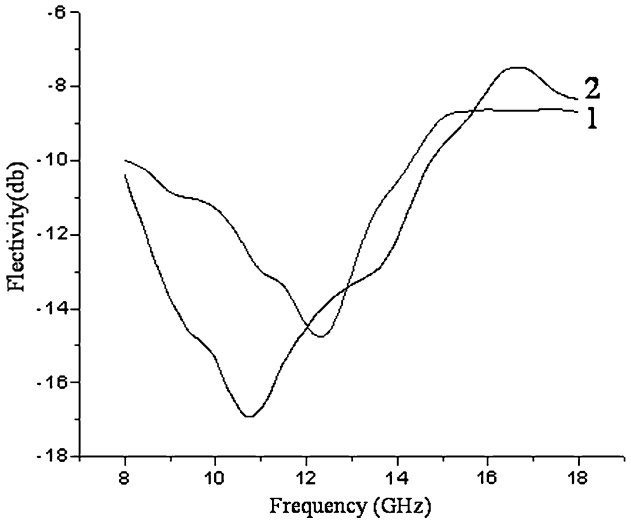

Fig. 9 The effect of spinning processes on the reflectivity of fiber with ferrite/20% bronze 1: in the sheath-part; 2: in the core-part

Conclusion

Sheath-core bicomponent fibers were prepared by a general melt-spinning method with polypropylene chips and ferrite and bronze particles. The results of the DSC thermogram indicated that the crystallinity of polypropylene including particles in the core-part was slightly increased with the particles content increase compared with that of pure polypropylene fibers. The MSER of fibers was rapidly decreased with the metal particles input. SEM micrographs showed that some particles had aggregated. The fibers filled with the ferrite/15 wt% bronze or ferrite/ 20 wt% bronze, had good radar absorbing effect. The fiber with fillers in the core-part obtained the lower reflectivity.

References

1. Vinoy KJ, Jha RM (1996) Radar absorbing materials from theory to design and characterization. Kluwer Academic Publishers, Boston
2. Stonier RA (1991) Sample J 27:9
3. Osamu F, Kei K (2002) Electr Eng Jpn 138:34
4. Im JI, Kim CW, Oh TS (1999) J Korean Ceramics 6:571
5. Yu XL, Zhang XC (2002) Mater Design 23:51
6. Sha Y, Jose KA, Neo CP (2002) Microw Opt Techn Let 32:245
7. Pomfret SJ, Adams PN, Comfort NP, Monkman AP (1999) Synt Met 101:724
8. Zabetakis D, Dinderman M, Schoen P (2005) Adv Mater 17:734
9. Kim SH, Seong JH, Oh KW (2002) J Appl Polym Sci 83:2245
10. Dhawan SK, Singh N, Venkatachalam S (2002) Synth Met 129:261
11. Brandrup J, Immergut EH, Grulke EA (1999) Polymer Handbook. John Wiley & Sons, New York
12. Sang YY, Sung HJ (2003) Polym Int 2:1053
13. Faez R, Gazotti WA, De Paoli MA (1999) Polymer 40:5497